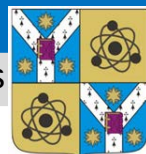




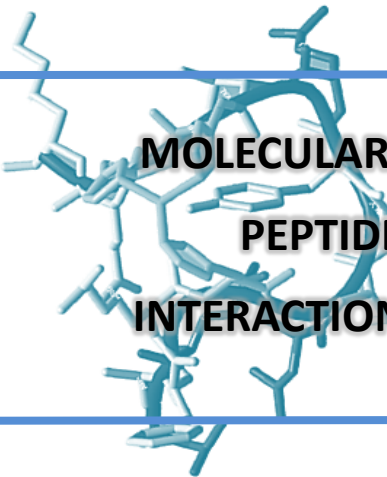
ALEXANDRU IOAN CUZA UNIVERSITY OF IASI

DOCTORAL SCHOOL OF THE FACULTY OF PHYSICS

Molecular biophysics and medical physics laboratory



PhD thesis summary



**MOLECULAR STUDY OF THE INFLUENCE OF
PEPTIDES STRUCTURE OVER THE
INTERACTION WITH LIPOPROTEIC SYSTEMS**

Scientific coordinator,
Prof. Dr. Tudor LUCHIAN

PhD,
Irina ȘCHIOPU

ALEXANDRU IOAN CUZA UNIVERSITY OF IASI
Doctoral School of the Faculty of Physics

We would like to cordially invite you to the Ph.D. thesis defence of miss
Irina ŞCHIOPU, entitled:

***“Molecular study of the influence of peptides structure over the
interaction with lipoproteic systems”***

which will be held on the 1st of September 2014, at 11:00, in FERDINAND
conference room, in order to obtain the PhD title in the fundamental field of Exact
Sciences – Physics.

The Ph.D. thesis committee consists of:

Prof. Dr. Diana MARDARE

Chairwoman

Director of the Doctoral School of the
Faculty of Physics
Alexandru Ioan Cuza University of Iasi

Prof. Dr. Tudor LUCHIAN

Scientific coordinator

Faculty of Physics
Alexandru Ioan Cuza University of Iasi

Prof. Dr. Nicoleta DUMITRAŞCU

Member

Faculty of Physics
Alexandru Ioan Cuza University of Iasi

C.S.I. Dr. Ioan TURCU

Member

INCDTIM, Cluj – Napoca

Conf. Dr. Dragoş GRIGORIU

Member

Gr. T. Popa University of Medicine and
Pharmacy, Iaşi



I would like to thank my scientific coordinator, Professor dr. Tudor Luchian and my colleagues dr. Aurelia Apetrei, dr. Loredana Mereuță and dr. Alina Asandei for their collaboration, trust and useful advices offered during my years of Ph.D.



I would like to thank Mrs. Prof. dr. Dorina Creangă and Mrs. Prof. dr. Nicoleta Dumitrașcu, also Ms. Lecturer dr. Loredana Mereuță for the guidance offered as members of the mentoring committee.



I would like to thank Mrs. Prof. dr. Nicoleta Dumitrașcu, Mr. scientific researcher dr. Ioan Turcu and Mr. Conf. Dr. Dragoș Grigoriu for their support as members of the examination committee.

TABLE OF CONTENTS

I. Aim of the study: Intelligent design of peptides – the key to new drugs with superior therapeutic properties	5
II. Antimicrobial peptides and their interaction with artificial lipid membranes	9
II.1. General characteristics of antimicrobial peptides	9
II.2. Destabilization mechanisms of the artificial lipid membranes. Types of transmembrane pores.....	15
II.3. The role of tryptophan amino acid in the peptide – lipid membrane interaction.....	19
III. Structural and functional features of the artificial lipid membranes. Electrical properties of the lipid membranes and their importance in modulating the peptides activity	24
IV. Structural and functional features of antimicrobial peptides used in the experimental studies	32
IV.1 Specific characteristics of antimicrobial peptide melittin.....	32
IV.2 Specific features of the synthetic analogs of the peptide HPA3NT0: Pep1, Pep2, Pep3.....	35
V. Single molecule interactions between protein nanopores and peptides	38
V.1. Interactions manifested at the level of the protein pore	38
V.2. Structural and functional features of the α -hemolysin protein pore	40
VI. Features of the peptides used in the single molecule studies	42
VI.1 Specific features of the chimeric peptide CA(1-8)MA(1-12).....	42
VI.2 Specific features of the human and rat 1-16 fragments of amyloid peptide	46
VI.3 Transition metals effect over the conformation of the amyloid peptides.....	52
VI.4 The chemical nature of the interaction between histidine amino acid and copper ions	56

VII. Methods and techniques applied in the study of the influence of peptide structure over the interaction with lipo-protein systems	61
VII.1. “Montal – Muller” technique of obtaining artificial lipid membranes	61
VII.2. Single molecule electrophysiology technique. The use of protein α – hemolysin as a nanosensor	65
VII.3. Preparation of liposomes.....	67
VII.4. The spectrofluorometric method.....	72
VII.5. Calcein fluorophor release assay method.....	76
VII.6. The quenching technique	79
VIII. EXPERIMENTAL RESULTS:	84
VIII.1. The study of melittin peptide interaction with lipid membranes	84
VIII.1.1. The effect of the dipole potential modifying agent phloretin over the activity of melittine peptide.....	84
VIII.1.2. The influence of ionic strength on the activity of the melittin peptide.....	91
VIII.2. The study of short peptides membrane activity with different position and spacial orientation of the tryptophan amino acid	94
VIII.2.1. The membrane activity of synthetic peptides analogs of HPA3NT0: Pep1, Pep2, Pep3 through electrophysiology method	94
VIII.2.2. The adsorption in liposomes of the peptides: Pep1, Pep2, Pep3 through fluorescence spectroscopy means.....	102
VIII.2.3. The kinetics of transmembrane pore formation of the peptides: Pep1, Pep2, Pep3 through a calcein efflux assay.....	109
VIII.3. The study of peptides conformational changes in the presence of physiologically relevant metals	114
VIII.3.1. Langmuir mathematical model applied for determination of the dissociation constant between the peptide and copper ions.....	114

VIII.3.2. The mathematical model developed for the study of association and dissociation reactions between the α – hemolysin pore and free- or Cu^{2+} -complexed CAMA peptide..... 120

VIII.4. Human versus rat (1-16) fragments amyloid peptide in interaction with copper ions study 136

VIII.4.1. Single molecule study of the copper ion-induced conformational differences of human and rat amyloid peptides..... 136

VIII.5. Study of the physiologically relevant metals effect on the spatial conformation of human amyloid peptide 1-16 fragment 151

VIII.5.1. Single molecule study of human amyloid peptide 1-16 fragment in the presence of Cu^{2+} , Zn^{2+} , Fe^{3+} și Al^{3+} . Dissociation constant, K_D , between human amyloid peptide and metals ions determination 151

Bibliography 152

I. Aim of the study: Intelligent design of peptides – the key to new drugs with superior therapeutic properties

Aim of the antimicrobial peptides study

The antimicrobial peptides are an essential part of the immune system that act against microbial infections. These are found both in plants, insects and in superior vertebrates. These natural peptides are basic compounds, with a primary structure of 12-50 amino acids, in current databases being registered over 800 such compounds. Some examples of such antimicrobial peptides along with their source would be: insect defensin A (fungi), cecropin A (insects), melittin (bee venom), magainin 2 (amphibians), tachyplesin 1 (crabs), α -defensin HNP-1 (humans).

Their composition in amino acids, amphiphile, the cationic electrical charge and their secondary structures, allow these peptides to absorb and to insert themselves in the lipid membranes in order to form transmembrane pores [1,2]. Although there were numerous attempts in elucidating their action mechanism through different such as classical transmembrane pores, toroidal pores or membranes [3], there still are debates concerning the mechanism of action on in vivo microorganisms.

In this study, we intended to investigate the influence of the position and geometric orientation of aromatic amino acids present in the primary structure of some antimicrobial derived from the peptide HPA3NT0 on the their mechanism of forming transmembrane pores in reconstructed lipid bilayers. The experimental results and their interpretation will offer a better understanding of lytic action mechanisms of these in vivo peptides, essential for assembling of new molecules derived from natural antimicrobial peptides, but with superior properties.

Aim of the interaction between peptides and transition metals study

In the last years, the interest towards the etiology of neurodegenerative disease has increased considerably, and one of the hypothesis proposed by the studies made until now in this direction indicate the disorder of the homeostasis at the brain level as main cause for inducing an abnormal conformation [4] of peptides and proteins involved in biological process of the organism. In the gran majority of cases, the wrong packaging of the peptides and proteins induces to the oligomerization, their aggregation and in the end to the formation of insoluble wounds [4]. A large variety of neurodegenerative disease are affected by the peptide and protein aggregation process, even though it is still unknown if the fibrils formation is the cause of the disease apparition or just a consequence.

In the study we aimed to develop a series of experiments in which to on one hand the conformation change of the amyloid peptides of human origin and murine after the complexation process with copper ions through electrophysiological techniques at one molecule level, and on another hand to prove the importance of the peptide primary structure in the wrong packaging of the mentioned in terms of the existing differences between the two the types of amyloid peptides. For this purpose we made use of the protein pore of ϵ α -HL in

order to test the interaction mode of amyloid peptides with this, in the presence and absence or copper ions, developing also a complex mathematical model that allows the quantitative analysis and the determination of essential parameters (i.e. dissociation constant) in describing the effects of copper ions over the amyloid peptides conformation. The relevance of applying this technique of study of the interactions at uni-molecular level stands in the easiness and elegance of its successful in the analysis at sub nanometric resolution for the DNA molecules and in various studies of molecular detection. The importance of implementing these techniques, described in detail in this paper, is presented by the possibility of describing molecular mechanisms that take place in one peptide only during its interaction with metal ions.

II. Antimicrobial peptides and their interaction with artificial lipid membranes

Numerous studies have described the influence of some important structural parameters of peptides: net electrical charge, helicity, intrinsic hydrophobicity, the hydrophobic moment, and the size of polar domains, respectively hydrophobic domains over membrane permeability effect, of the antimicrobial and hemolytic effect. The experiments show that these parameters can constitute a strong basis in the peptides structure, correlated with their antimicrobial activity. The predominance of a permeability mechanism is determined by the cumulated effect of the absorption and membrane permeability stages. The main characteristics that determines the activity and specificity of antimicrobial peptides are: primary sequence, secondary structure, helicity, the hydrophobic moment, hydrophobicity, the hydrophobicity angle and the electric charge of the peptide.

Until now there have been described 2 different types of ionic canals formed by the aggregation of cytotoxic peptides: *classic pores* („barrel stave”) whose interior is formed only by polar parts of the peptides and *toroid pores* for whose interior structure there are polar heads of lipids that contribute which enter the membrane structure. (Fig. II.2.1).

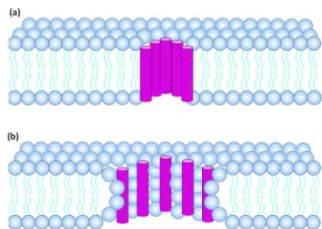


Fig.II.2.1. Schematic representation of the forming models of the transmembranary pores. (a) Classic pores model; (b) Toroid pores model [10]

A different interaction mode with the lipid bilayer would be represented by the *carpeting mechanism*, according to which the peptides are accumulated at the interface bilayer/aqueous medium under the form of a “carpet” and, when a threshold value of the monomer concentration is surpassed, the membrane is permeability and disintegrated in a manner similar to the detergent action, without the formation of distinct ionic canals (Fig. II.2.2).

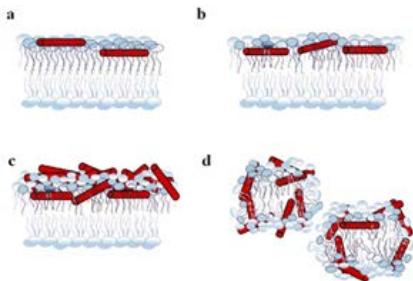


Fig. II.2.2. Schematic representation of the disruption model of the cellular membrane through the carpeting mechanism. The α -helix structured peptides are absorbed initially at the interface membrane/ aqueous medium (a) then they are accumulated (b) parallel oriented at the membrane surface. The continuous accumulation of peptides at the bilayer level leads to the „covering (carpeting)” with peptides (c) and finally, when a critical concentration is reached, to its disintegration (d) [11].

The high resolution investigation of the protein structure inserted in the lipid membranes and recent studies on the role of individual amino acids in mediating the interactions proteins – lipids have shown that the polar residues – aromatic, tryptophan (Trp) and tyrosine (Tyr), show a specific affinity for the lipid region present at the interface membrane/ aqueous medium. The interface membrane/ aqueous medium represents a relatively big part of the total width of the lipid bilayer and represent a complex chemical medium, that offers many possibilities for noncovalent interactions with the lateral chains or the peptides and proteins. This interface represents a polarity gradient, from very nonpolar in the immediate region of hydrocarbon queues that form the hydrophobic core of the, until very polar, close to the aqueous phase. The carboxyl grouping of lipids, phosphocholine grouping, and also the water molecules around the polar ends of phospholipids offer the possibility of interaction of dipole – dipole type, cation – π , the forming of strings of hydrogen with lateral chains of amino acids from the peptide and protein structure [12,13].



Fig.II.3.1 The interaction cation- π between a random cation and an aromatic benzene ring [adapted from UC Davis ChemWiki].

The interaction cation – π represents a strong interaction of non-covalent nature between the orbital electrons π (in which the electronic density is distributed uniformly onto and beneath the molecule plan) and one cation found nearby. In the case of interactions type cation – π exhibited at the interface of the lipid bilayer and aqueous medium, the connection is formed between the indole ring of the tryptophan amino acid and the nitrogen electrically charged positive from the choline group of the polar ends of phospholipids that compose the lipid bilayer.

The hydrogen connections are manifested between the hydrogen from the NH grouping of the indole ring of tryptophan and the oxygen from the carboxyl grouping (C=O). The strength of these connections depends on the type of phospholipids from the membrane, energy calculations from molecular dynamics have shown that the prevalence of cation – π

interactions increases in the case of lipids for which the cation nitrogen is more exposed (e.g.: POPE, 1-palmitoyl-2-oleoylphosphatidylethanolamine, where the nitrogen is tied with only three atoms of hydrogen, as against POPC, 1-palmitoyl-2-oleoylphosphatidyl-choline, where the nitrogen is connected to three groupings CH) [14].

III. Structural and functional features of the artificial lipid membranes. Electrical properties of the lipid membranes and their importance in modulating the peptides activity

The biological membranes are polymeric structures build mainly from lipids and proteins, with an essential role in maintaining the cellular integrity through the fact that it is a very selective permeation barrier between the intra and extracellular mediums. These serve as support for a vast class of membrane proteins that are practically solubilized in the lipid bilayer and that have an essential role in the processes of cellular transduction, cellular communication, DNA replication, in the cellular recognition processes, etc. Although the characteristic of all cells that enter the composition of living matter is its functional and structural diversity, all bio membranes are planar structures, with widths between 60Å and 100Å, formed mainly from lipids and proteins. Moreover, the bio membranes are non-covalent molecular superstructures organized under the form of lipid bilayer whose monolayers al present asymmetry.

Generally, it may be said that the electrical profile of the bio membranes is composed of: the contribution of the transmembrane contribution, the dipole potential and the different surface potential between the 2 faces of the membrane. While the transmembrane potential results from the charge gradient on one part and the other of the membrane and the surface potential is given by the net charge excess present on the membrane surface, the dipole potential of the membrane has its origins in the molecular dipoles localized at the lipid molecule level.

The dipole potential (ψ_d) (Fig.III.4) represents the third component of the total transmembrane potential. The structural studies of the biomembranes revealed the fact that the origin of the dipole potential is given by two main factors and namely: on one hand the orientation of the dipolar groupings localized in the lipid molecules (the dipole corresponding to the carbonyl grouping from the ester connection and the dipole of the terminal end ($P^- - N^+$), on the other hand the dipolar moments corresponding to the water molecules situated at the interface membrane/aqueous medium.

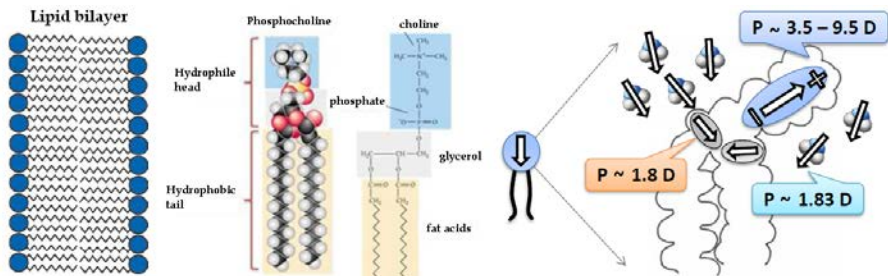


Fig.III.4. Schematic representation of a lipid bilayer (a) made of phospholipids whose structure present a polar region (choline-phosphate- glycerol) and two hydrophobe queues of hydrocarbon (fat acids) (b) Schematic representation of the dipole potential ψ_d , correlated with the existance of the dipolar moments different than 0 existing in the hydrophilic edges of lipids that enter the composition of biological membranes ($P^{\delta-} - P^{\delta+}$), ($C^{\delta+} - O^{\delta-}$) and the dipolar moments of the water molecules.

In the current literature there are known certain molecules that can modulate the amplitude of the membrane dipole potential when they get to the membrane surface. Between these, phloretin has the ability to decrease the amplitude of the dipole potential. Phloretin is a weak acid, it has the value $pK_a = 7.3$ and its active forme is the neutral with a $pH < 7.3$.

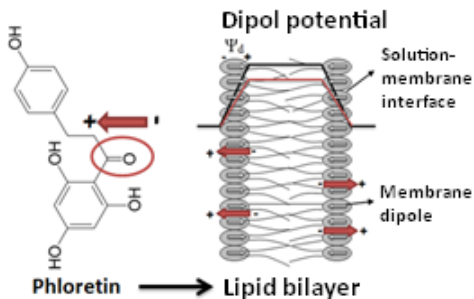


Fig.III.6 Representative schema for the molecule absorption by phloretin at the interface membrane – aqueous medium. The chemical structure of the phloretin molecule, as well as the corresponding dipole moment given by the carboxyl grouping (C=O) is represented on the left, and the lipid bilayer is represented on the right together with the dipole potential given by the polar edges. The direction in which the phloretin molecules are being absorbed is with the dipol moment reversely oriented against the one of the polar edges, leading to a decrease of the dipole membrane potential.

IV. Structural and functional features of antimicrobial peptides used in the experimental studies

Melittine (*Apis Mellifera*): H_2N -Gly-Ile-Gly-Ala-Val-Leu-Lys-Val-Leu-Thr-Thr-Gly-Leu-Pro-Ala-Leu-Ile-Ser-Trp-Ile-Lys-Arg-Lys-Arg-Gln-Gln-CONH₂

HPA3NT0 analogues (*Helicobacter pylori*): Phe-Lys-Arg-Leu-Glu-Lys-Leu-Phe-Ser-Lys-Ile-Trp-Asn-Trp-Lys

Pep1: Leu-Lys-Arg-Leu-Gln-Lys-Leu-Leu-Ser-Lys-Ile-**Trp**-Asn-Lys-**Trp** - NH₂
Pep2: **Phe**-Lys-Arg-**Trp**-Gln-Lys-Leu-Leu-Ser-Lys-Ile-**Trp**-**Trp**-Lys-Asn - NH₂
Pep3: Leu-Lys-Arg-Leu-Gln-Lys-Leu-Leu-Ser-Lys-Ile-**Trp**-**Trp**-Lys-Asn - NH₂

V. Single molecule interactions between protein nanopores and peptides

The translocation process through proteins, of nanometric dimensions, inserted in the membranes of eukaryotic cells is significant for maintaining their functions. In the last years, the interest for such processes has increased apprehending the potential of some proteins of being used in the biotechnology domain, as bimolecular detection systems. Thus, this technique was used in the characterization of some particle suspensions [15-17], DNA sequencing [18,19] or the detection of the conformational peptide changes [20, 21].

In brief, when a molecule translocates through a protein pore of nanometric dimensions, inserted into a lipid membrane which separates two compartments with electrolytic solution, this will block the access of ions into following the route to the interior of the pore, leading to a decreased of the initial ionic current, corresponding to the free pore. The profile and succession of ionic current fluctuations generated by the passing of various types of molecules through one protein pore only can offer useful information regarding their structural characteristics.

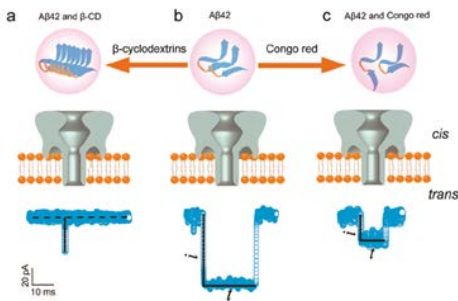


Fig.V.1.1. Representation of an only proteic pore of α -HL inserted in the lipid membrane. The amyloid-beta peptide presented in the presence and in the absence of β -cyclodextrin ($A\beta$ 42-CD) or of the molecule of red congo. (a) Representation of the ionic current blockages due to the interaction between the pore and the complex $A\beta$ 42-CD. (b) Representation of ionic current blockages due to the interaction between the pore and the complex $A\beta$ 42. (c) ionic current blockages due to the interaction between the pore and the complex $A\beta$ 42-congo red. [22]

α -hemolysin (α -HL) is a monomeric protein of 33.2 kDa soluble in water, secreted by the bacteria *Staphylococcus aureus*, which presents auto assembly properties, forming heptamer ionic canals in the lipid or artificial membranes. (Fig.V.2.1).

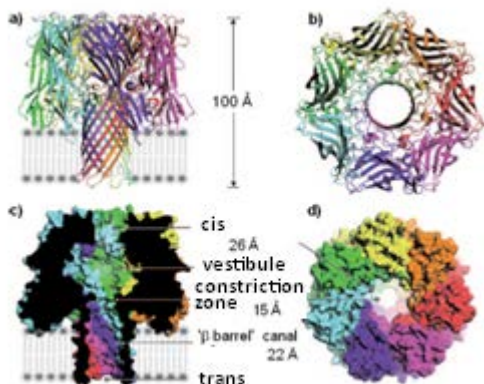


Fig.V.2.1 (a) Lateral view of the heptamer complex of α -hemolysin which shows the insertion mode in the membrenary lipid bilayer. The complex has a lenght and a diameter of approximately 100 Å. (b) View of α -hemolizinei from the *cis* part of the lipid membrane (c) and (d) Longitudinal section respectively the ‘space-filling’ model of the protein that shows the interior diameter of its canal on different positions. Each color represents a different monomer of α - hemolysin [23].

The crystalline structure of this protein is well known [24]. Due to the possibility of introducing numerous local mutations in the structure α -HL, the protein is a good candidate for a wide range of applications. Taking into account the particular biological importance of the interaction between the peptides and protein pores, there were realized many studies that investigate the partitioning of the peptides in the protein pore of α -HL [24-33].

VI. Features of the peptides used in the single molecule studies

VI.1 Specific features of the chimeric peptide CA(1-8)MA(1-12):

CA(1-8)MA(1-12) – formed by joining the first eight amino acids of the peptide *cecropin A* with the first twelve amino acids of the peptide *magainin 2*:

Lys-Trp-Lys-Leu-Phe-Lys-Lys-Ile-Gly-Ile-Gly-Lys-Phe-Leu-**His**-Ser-Ala-Lys-Lys-Phe-NH₂

VI.2 Specific features of the human and rat 1-16 fragments of amyloid peptide:

uman - A β (1-16):

Asp - Ala - Glu - Phe - Arg - **His** - Asp - Ser - Gly - Tyr - Glu - Val - **His** - **His** - Gln - Lys

murin - A β (1-16):

Asp - Ala - Glu - Phe - Gly - **His** - Asp - Ser - Gly - Phe - Glu - Val - Arg - **His** - Gln - Lys

VI.3 Transition metals effect over the conformation of the amyloid peptides

From the studies conducted until the current date it is clearly revealed that the disorder of the transition metal homeostasis present in the organism play an important role in the etiology of the neurodegenerative disease Alzheimer. Thus, the elucidation of the structural details that are at the basis of the interaction between these metals and the amyloid peptides would facilitate the understanding of the apparition of neurotoxicity and design of some chemical substances that would have a therapeutic action. The studies conducted over the conformation changes of these peptides induced by zinc ions indicate the involvement the three residues of histidine (His6, His13 and His14), like in the case of copper. The forth coordinative connection being still unknown, some studies have proposed possible candidates: the oxygen of the glutamic acid (Glu11), the N – terminal edge when it is acetylated or the aspartic acid(Asp1), when the N-terminal edge is not acetylated [34]. Comparative studies, of nuclear magnetic resonance, ¹H RMN, that concerns the effect of zinc ions over the peptide segment A β (1-28) of human origin and murine dissolved in water or SDS (sodium dodecyl sulfate), at neutral pH [35] have shown that glutamic acid (Glu11) would have the highest potential of creating a forth coordinative connection with the zinc ions, and the difference of one histidine (H13R) between the two peptides would be responsible for the more stable conformation taken by the peptide of human origin, the one that contains three histidine amino acids, than the other, that presents only two histidine.

VI.4. The chemical nature of the interaction between histidine amino acid and

Copper ions

The copper levels found at neuronal level is significantly increased at patients that are already in an advanced stage of the Alzheimer disease as against the healthy patients. The numbers indicate copper values of $4.4 \pm 1.5 \mu\text{g/g}$ in the case of the control sample, to $19.3 \pm 6.3 \mu\text{g/g}$ in the case of the test sample, reaching even to values of $30.1 \pm 11 \mu\text{g/g}$ in analysis in the middle of the senile plaque [36].

Histidine (His) is one of the 20 main amino acids that are in structure of proteins and peptides. It contains an imidazole ring as lateral chain, aromatic at any value of the pH. It contains six electrons π : four from two double connections and two from the nitrogen, the las ones being pair of free electrons that can contribute on the forming of coordination connections with metals. The free electrons of the nitrogen from the amine grouping contributes to the aromatic character of the imidazole ring. Through the hybridization of the orbital 2sp and its on from the hydrogen atom, it does not have any more free electrons to form coordinative connections with metals. On the other hand, the nitrogen from the imine grouping, which has two sigma connections and one pi connection is already in a hybridized state 2sp.

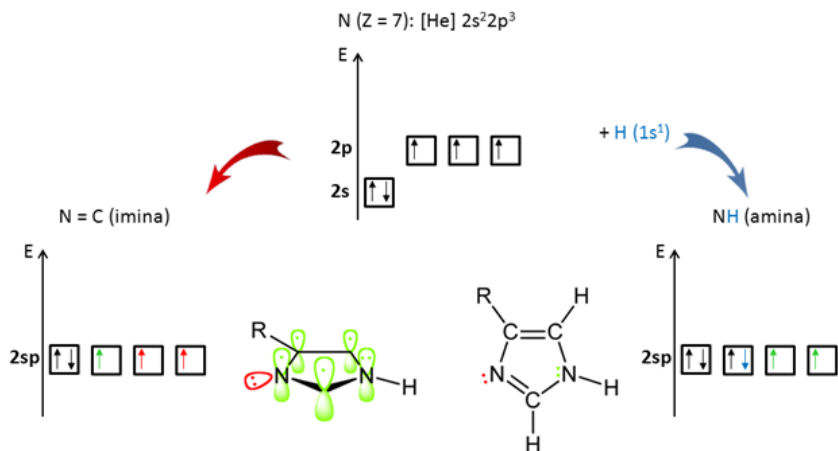


Fig.VI.4.2 The electronic configurations and electronic groupings on energetic sublevels of the simple nitrogen atom and in those amine groupings (right) and respectively imine (left) of the amino acid histidine. For the simplicity of the representation the groupings amine ($-\text{NH}_2$) and the carboxylic acid (COOH) that enter polypeptide chain of a peptide noted with R, having an interest only in the lateral chain of the amino acid histidine (imidazole ring). In the case of the amine grouping, the hybridization of the energetic level is made at the interaction with the hydrogen atom (having only three connection of σ type), contrary to the imine grouping where the energetic level is already hybridized (having already two connections of σ type and one π type).

So the pair of free electrons is already on the 2sp orbital hybridized and with which may contribute to the coordinative connection with the copper ions, more exactly the orbital 4sp. For this reason, the copper ions are preferentially connecting to the nitrogen atoms from certain amino acids, such as the histidine from the main structure of the peptide β – amyloid.

VII. Methods and techniques applied in the study of the influence of peptide structure over the interaction with lipo-protein systems

“Montal – Muller” technique of obtaining artificial lipid membranes. The monitoring the dependent voltage channels formed by cytotoxic peptides in lipid bilayers represents one of the most useful investigation technique for the formation and the stability of transmembrane pores induced by these at the level of biological cellular membranes. The amplitude of the electricity mediated by the pores formed by the cytotoxic peptides in the artificial membranes represent a measure of the penetration capacity of the biomembranes by these peptide molecules. When the peptides are absorbed at the interface bilayer/aqueous medium, they are inserted in the hydrophobic core of the bilayer, forming transmembrane aqueous pores that can be monitored by recording the electricity changes that appear in the system upon applying a deference of potential on both sides of the lipid membrane. (Fig.VII.1.1)

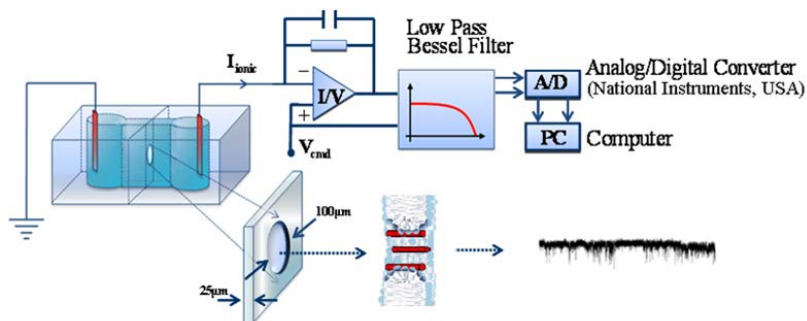


Fig.VII.1.1 Schematic representation for the components of the experimental device used for realizing the artificial biomembranes. The lipid bilayer is formed at the aperture level of 100 μm of the teflon film with a width of 25 μm detailed view of the biomembrane formed at the level of teflon partition which separates the two teflon tanks, in which, for exemplification, it is considered inserted an ionic channel of alamethicin. The electricity was detected and amplified with an integrated amplifier Axopatch 200 B (Molecular Devices, USA) setup on the module fixed voltage, through two Ag/AgCl electrodes. The data acquisition was realized with an acquisition plaque NI PCI 6221 on 16 bits (National Instruments USA), with an acquisition frequency of 30 kHz in the graphic medium LabVIEW 8.20.

Single molecule electrophysiology technique. The use of protein α – hemolysin as a nanosensor The recording of electricity fluctuations mediated by membrane ionic channels through molecular electrophysiology techniques is essential for the direct viewing of the molecular transitions realized by one ionic channel and to study the phenomenon of ionic transport or of some little molecules through these ionic channels. These transitions have a purely stochastic character so, in describing the behavior of these molecules are important in estimating the exact number of molecular stages (of types “closed” and “open”) through which an ionic channel can pass, determining the transition rates between these states and also the analysis of the ionic transport processes mediated by these channels.

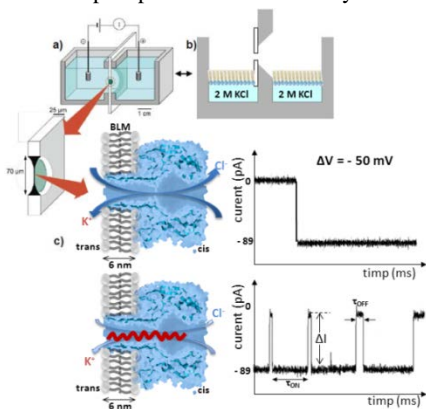


Fig.VII.2.1 Specific fluctuations of the ionic current through a single proteic pore of α -HL induced upon the addition in the *trans* part of the lipid membrane of the peptides, recorded at a value of the applied potential difference of -50 mV, observed on the form of stair type alterations of the ionic current to more positive values of it.

The peptides rapidly interact with the constriction area of the protein pore, leading to full or partial blocking events, with a duration long enough to be able to monitor them. The amplitude values of the blockages of the protein pore against the peptide are given by the conformation in which the peptide is found, it may block completely the pore in the restriction area, which suggests a more voluminous special layout, or it may partially block the pore, which indicates a linear arrangement of the peptide when it passes through the pore.

Preparation of liposomes. The liposomes, the most common nanoparticles made of lipid molecules, can be represented by a sphere which's diameter varies between 30 nm and 10 μm . g bilayers become fluid and grow in size. The hydrated lipid layers are detached during the agitation process and their edges are getting closer in order to avoid the contact of water with the hydrophobic core of the bilayer, forming multilamellar vesicles. In order to reduce the dimension of these vesicles, it is necessary to have an energetic contribution under the form of sonic energy (sonication) or mechanic energy (extrusion), this way resulting small unilamellar vesicles (SUVs).

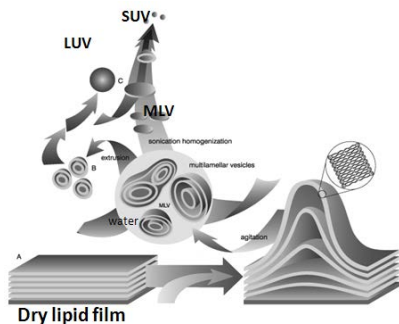


Fig.VII.3.3 Schematic representation of the forming stages of the small unilamellar vesicles (SUV). Generally, the obtaining procedure of the liposomes involves: preparing the lipids for hydration, hydrating through agitation and bringing them to a homogenous distribution of the vesicle dimension through sonication.

The spectrofluorometric method. The fluorescence spectroscopy is an electromagnetic spectroscopy type that analyses the fluorescence of a study sample. This type of analysis involves the use of a light fascicule, usually with ultraviolet rays, that excite the electrons of the molecules from some certain compounds which leads to the light emission with a lower energy than usual, but not necessarily, in visible light

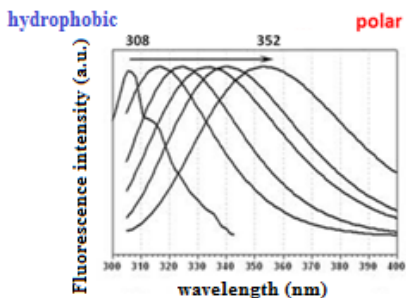


Fig. VII.4.4 If initially the tryptophan is found in a solvent polar and then is passed in a hydrophobe environment (apolar), the emission spectrum will be moved towards the blue region of the wavelength.

Tryptophan has an absorption spectrum of 280 nm, while the emission spectrum maximum varies between 300 and 350 nm, according to the solvent's polarity [37,38]. The existing Tryptophan in the primary structure of the proteins may, therefore, be used for estimating the nature of the environment where it is found. According to the polarity, flexibility and chemical nature of the environment on which the tryptophan is found, this will interact differently at the redistribution of the electronic density in the indole ring of the amino acid.

Calcein fluorophore release assay method. The calcein fluorophore is presented under the form of orange colored crystals, having the excitation wavelength of 495 nm, respectively the maximum emission spectrum of 525 nm (Fig.VII.5.1). In the specialized literature it is specified the fact that the calcein fluorophore quenches the fluorescent emission even at concentration levels less than 100 mM [39]. During the experiments, the calcein was solubilized in a solution with a concentration of 50 mM, which insured the quenching. The lipid systems used in these experiments are spherical liposomes formed through the same protocol as the one described in the subchapter VII.3., hydrated with the help of the calcein solution. In order to eliminate calcein from the external environment of the small unilamellar vesicles thus formed, the liposome suspension was subjected to a chromatographic separation process on columns with gel [40]. The elimination of the free calcein from the lipid suspension was made using PD-10 columns with a content of Sephadex G-25 gel, that insures the separation of the compounds with a high molecular mass against those with low molecular mass. The cytotoxic peptides are inserted in the lipid bilayer and form transmembrane pores through which the calcein, found in the interior with a concentration that insures the quenching, is freed in the external environment and emits fluorescently. The real time evolution of the fluorescence intensity can be correlated with the kinetics of the pore formation by the studies cytotoxic peptides.

The quenching technique. Quenching refers to any process that induces the intensity decrease of fluorescence of certain substances called fluorophores after their interaction with other molecules, called quencher molecules.

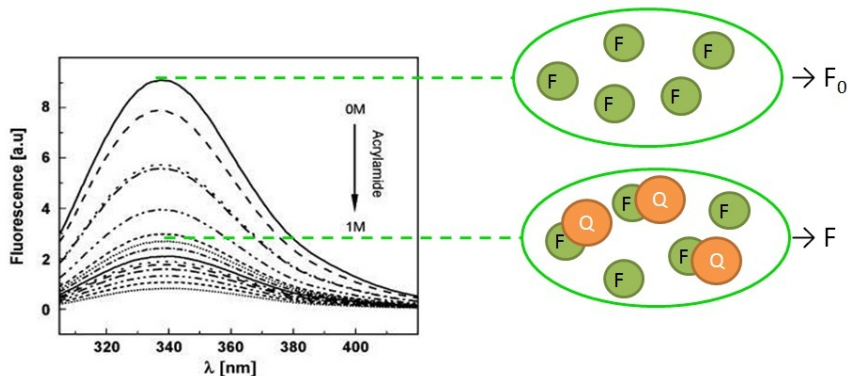


Fig.VII.6.3 Graphical representation of the emission spectrum of the PV2 protein where the emission intensity decrease is observed upon adding a concentration up to 1M of acrylamides [44].

There are numerous quencher molecules that can act on the fluorophores, extinguishing their fluorescence emission through different mechanisms: oxygen, that interacts with approximately all fluorophore types, heavy ions, histidine and cysteine residues, amines, metal (Cu^{2+} , Pb^{2+}). Acrylamide is a white chemical compound, odorless and toxic, with a high solubility in water (2.04 kg/L at 25 °C), but also in acetone, ethanol or chloroform, polar but neutral from the electric point of view and it is not inserted in the hydrophobic core of the phospholipid membrane. The acrylamide molecules interact with the excited fluorophores inducing the fluorescence decrease through collisional processes [41 - 43]. The quenching technique is useful in numerous applications, such as measuring the fluorescence of the transmembrane protein marked fluorescent may offer information regarding the exact location of it in the membrane domain.

VIII. EXPERIMENTAL RESULTS

VIII.1. The study of melittin peptide interaction with lipid membranes

VIII.1.1. The effect of the dipole potential modifying agent phloretin over the activity of melittin peptide

Fluorescence quenching experiments results. In our study we highlighted the effect of phloretin modifier agent at the artificial cell membrane surface (SUVs), on the melittin antimicrobial peptide adsorption using the fluorescence spectroscopy method. This technique involves the tracking the decrease in fluorescence emission intensity of the tryptophan amino acid, present in the melittin peptide sequence, after it interacts with the acrylamide quencher molecules. The spectral analysis is based on the emission maximum decreases of the tryptophan fluorescence intensity, as a result of acrylamide concentration increasing, both in the case of the liposome suspension and for the liposomes with phloretin added. The acrylamide molecules are

useful in detecting of the peptide environment, such giving us an indication of the depth in the bilayer that are adsorbed monomers peptide.

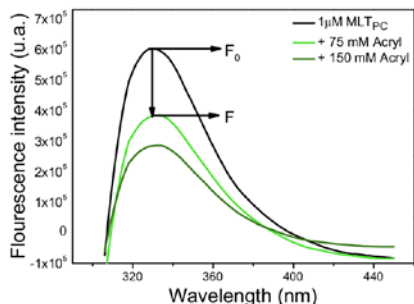


Fig.VIII.1.1.2 Emission spectra of 1 μM melittin peptide adsorbed in simple liposomes (black) and the fluorescence intensity decrease of the melittin emission spectra after the addition of 75 mM (green) and 150 mM acrylamide (red).

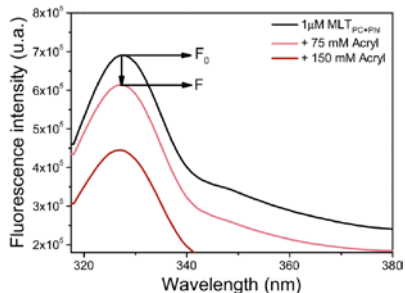


Fig.VIII.1.1.3 Emission spectra of 1 μM melittin peptide adsorbed in liposomes with 20 μM phloretin molecules (black) and the fluorescence intensity decrease of the melittin emission spectra after the addition of 75 mM (cyan) and 150 mM acrylamide (magenta).

It is observed, that for the same concentration value of acrylamide (e.i. 75 mM), the decrease in the maximum of fluorescence emission spectrum is lower in the case of the liposomes that contain the phloretin molecules. This is due to the fact that the tryptophan amino acid is less exposed to the quencher molecules, so the probability of the collisional processes to happen are lowered. The quantitative analysis of the experimental data and the linear fit applied using the Stern – Volmer equation offers the possibility of determine the parameter that gives information about the degree of adsorption of the peptide into the lipid systems (K_{SV}).

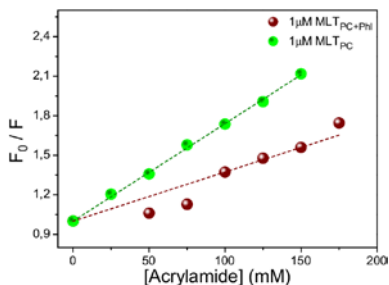


Fig.VIII.1.1.4 Linear fitting of the experimental data obtained for simple liposomes (green) and liposome with phloretin (brown). The slope of the linear fit represents the Stern – Volmer constant, expressing the degree of exposure of the peptide. The decrease in fluorescence intensity due to acrylamide quenching effect is expressed through the ratio of the maximum of fluorescence intensity, in the absence of the quencher, to the maximum of fluorescence intensity after the addition of different concentrations of quencher.

MLT in:	K_{SV} (M^{-1})
SUV	7.41 ± 0.07
SUV+Phl	3.73 ± 0.30

The analysis of the constant values obtained show the fact that the melittin peptide are more adsorbed into the membrane of the liposomes in which phloretin molecules were inserted. The

phloretin molecules modify the electrical properties of the lipid membrane by decreasing the dipole potential and promoting the adsorption of the peptide melittin, making the interaction energetically advantageous.

Calcein release experiments results. The purpose of this study was the investigation of the phloretin molecules effect over the insertion and pore formation of the melittin peptide into the lipid membrane. The kinetics of transmembrane pore formation were monitored by recording the time-variation in the emission fluorescence maximum of the calcein fluorophore released in the aqueous medium. Thus, the initial concentration encapsulated into the liposomes was 50 mM, sufficient for the selfquenching effect to take place. After the addition of 3 μM melittin peptide, the emission fluorescence was recorded at an emission wavelength of 520 nm. The experiments were performed at a concentration of 100 μM liposomes suspension, with and without the presence of 20 μM phloretin solution.

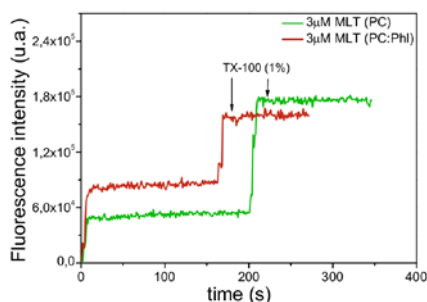


Fig.VIII.1.1.5 Real time evolution of the calcein fluorescence intensity, as a result of its release from the liposomes inner, made of phosphatidylcholine (green trace) and phosphatidylcholine with phloretin (brown trace), after the transmembrane pore formation by the melittin peptide.

The analysis of the experimental data obtained shows that the presence of phloretin molecules into the lipid membrane induces a higher calcein release as a direct consequence of the increase in the number of transmembrane pore formation. The increase in the probability of interaction between the melittin peptide and the lipid membrane of the liposomes is due to the decrease in the free energy cost necessary for the peptide to cross the bilayer and form pores. This is made possible by influencing the dipole potential of the lipid membrane by introducing in the system modulating agents like phloretin.

VIII.1.2. The influence of ionic strength on the activity of the melittin peptide

We recorded in real time the variations in fluorescence emission intensity of the calcein fluorophore while it was released from within the liposomes. The experiment were performed on lipid systems made of phosphatidylcholine (100 μM) or lipid systems made of phosphatidylcholine (100 μM) and phloretin (20 μM). The concentration used for the melittin peptide was 3 μM , and only the ionic strength was modify, for a low concentration it was used 50 mM KCl and for a high one, 200 mM KCl, both buffered with 10 mM HEPES at a pH pf 7.3.

The excitation wavelength used was 495 nm, characteristic to the maximum of absorption of the calcein fluorophore.

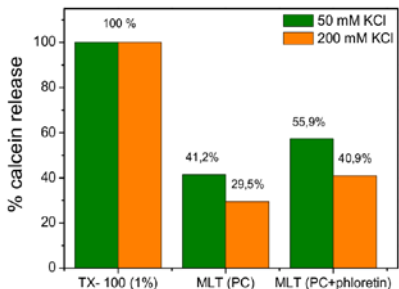


Fig. VIII.1.2.1 Calcein release percentage after the insertion of the melittin peptide into the liposomes simple membrane (PC) and with phloretin membrane (PC+phloretin) at different ionic strength of the physiological solution: 50 mM KCl (green) and 200 mM KCl (orange). The maximum release was obtained by adding the nonionic surfactant TX-100 (1%) that acts like a detergent inducing the liposomes structures disruption.

The experiments showed a decrease in melittin activity into artificial membrane, under conditions of higher ionic strength. This can be explained by the fact that in the presence of a high concentrations of ions in solution, the peptides cationic residues will be in competition with the positive ions of salt, for the same sites of interaction, namely the lipid polar heads. Also, the positively charged amino acids of peptides will be stronger screened into a solution with higher ionic strength, so that the electrostatic interactions between peptide and the phosphate groups of lipids will be diminished.

VIII.2. The study of short peptides membrane activity with different position and spatial orientation of the tryptophan amino acid

VIII.2.1. The membrane activity of synthetic peptides analogs of HPA3NT0: Pep1, Pep2, Pep3 through electrophysiology method

Electrophysiology experiments were carried out in the folded bilayer membranes system obtained with Montal–Mueller technique. A symmetrical lipid bilayer was formed from lipid mixtures containing POPC/DOPG (85:15, w/w) dissolved in pentane., which made the bilayer slightly anionic in order to facilitate the insertion of the cationic peptides used in this experiments. In a minimalist model and given that the dipolar moment and charge of pep1 and pep2 are similar, the difference in the voltage-dependence of peptide-induced activity in planar membranes of pep1 and pep2, reflects the larger energy cost of translocation of pep2 across the hydrophobic bilayer core as compared to pep1, due to its flanking W4 and W12.

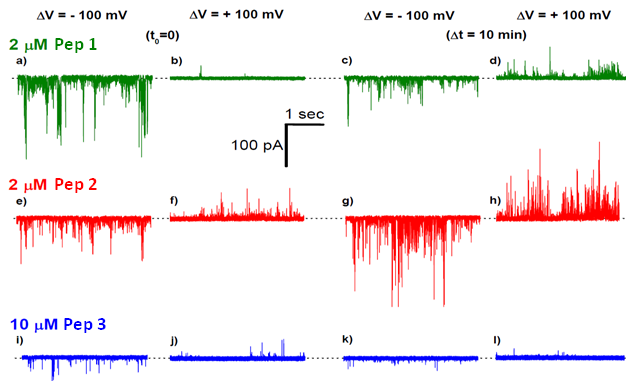


Fig.VIII.2.1.1 In panels a), b) and respectively e), f) are shown representative traces which illustrate pep1 and pep2 (2 μM) activity in planar lipid membranes clamped at -100 and +100 mV. And in panels i) and j) the activity of pep3 at a concentration of 10 μM . Right panels show recordings after 10 min. The closed state of peptide oligomers is denoted by the dotted line, while downward (-100 mV) and upward (+100 mV) spikes designate the electrical currents mediated by peptides-induced pores.

Within the framework of a simplified thermodynamic system, whereby only two states exist for the peptide interacting with the membrane bilayer (i.e., interfacial adsorbed - IFC and transmembrane inserted-TM), to derive the free energy of insertion we fitted the voltage-dependent curves with a Boltzmann-like equation. We therefore propose that the difference in pep1 and pep2 activity stems from the voltage-independent energy factor, that may be associated to different barrier heights associated to the insertion of F1 and W4 residues of pep2. Since W12 and W15 are situated very close to the C-terminus of pep1, given their affinity of the membrane interface and considering that the peptide N-terminus is uncapped, it is likely that during the insertion process these amino acids remain anchored to the cis membrane interface, whereas the negatively applied potential on the trans side would draw the positively charged N-terminus head-on across the membrane, from the cis- to the trans side. The same physical rationale applies to pep2, i.e. its C-terminus stays anchored to the cis membrane interface through Trp12 during the insertion process. The Boltzmann fit performed for both pep1 and pep2 allowed to estimate the barrier to insertion of monomeric peptides into lipid bilayer (i.e.,

$\Delta G_{TM-IFC}^{non-el; pep1} = -3.5 \text{ kcal/mol}$ and $\Delta G_{TM-IFC}^{non-el; pep2} = -3.3 \text{ kcal/mol}$), and results matched those reported previously for analog sequences which undergo transition from a surface-bound to a transmembrane orientation. By keeping in above equation the voltage-dependent part (αV) of the difference in free energy invariant for both pep1 and pep2, the offset

$$P_{TS} = \frac{1}{1 + e^{\frac{\alpha V + \Delta G_{TM-IFC}^{non-el.}}{RT}}}$$

in the voltage-independent part of the free energy change associated to the transition between the two global states of the peptides ($\Delta G_{TM-IFC}^{non-el.}$)

quantifies properly the supplementary energy ($\sim 0.2 \text{ kcal/mol}$) needed to bury the supplementary aromatic residue from pep2 within the bilayer hydrophobic core, namely F1 and W4. In a simplistic model, and motivated by energy and geometric arguments, we assume that the most plausible orientation of pep2 in its interfacial state (IFC) is the most stable one, e.g. with F1, W4

and W12 pointing towards the membrane head group region of the cis membrane monolayer, and as the insertion progresses, W12 remains locked at the cis interfacial region.

VIII.2.2. The adsorption in liposomes of the peptides: Pep1, Pep2, Pep3 through fluorescence spectroscopy means

Interaction between the peptides and unilamellar vesicles present in suspension at concentrations ranging from 20 μM to 300 μM , were studied by monitoring the lipid-induced spectral blue shift $\Delta\lambda$, corresponding to the change in wavelength of the emission fluorescence signal maximum compared to the lipid-free spectrum. The spectral blue shift is caused by the less polar environment experienced by the tryptophan residue when adsorbed in the lipid membrane interfacial layer. Taking into account the fact that the blue shift is proportional with the adsorbed peptide concentration, we can apply the mathematical model that lead us to the association constants of the peptides to the liposomes.

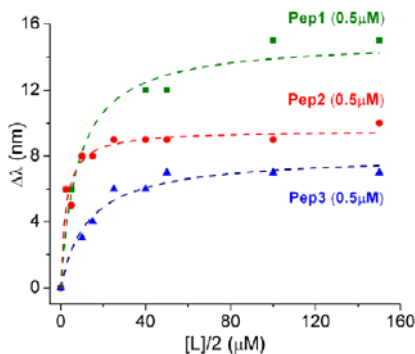


Fig.VIII.2.2.3 Binding isotherms for pep1 (filled squares), pep2 (filled circles) and pep3 (upward triangles) to liposomes. Dashed lines are non-linear hyperbolic fit according to the equation 3 ($R_2 = 0.936$ for pep1, 0.948 for pep2, and 0.968 for pep3) to obtain estimates of the maximum fluorescence emission blue shift ($\Delta\lambda_{\text{max}}$) and the apparent binding constant (K_a).

$$\Delta\lambda = \Delta\lambda_{\text{max}} \cdot \frac{K_a \cdot [L]}{1 + K_a [L]}$$

The values of $\Delta\lambda$ were displayed against the lipid concentration and apparent binding constant (K_a) as well as the maximum fluorescence emission blue shift ($\Delta\lambda_{\text{max}}$) were extracted from the non-linear hyperbolic fit according to the equation. Also, the free energies corresponding to the partition of the peptide into the hydrophobic core of the lipid bilayer were calculated: pep1 (-9.29 kcal/mol), pep2 (-10.02 kcal/mol) și pep3 (-9.01 kcal/mol).

VIII.2.3. The kinetics of transmembranare pore formation of the peptides: Pep1, Pep2, Pep3 through a calcein efflux assay

In the following, a fluorescence spectroscopy assay was proposed in order to monitor the transmembrane pore formation into the lipid membrane by the short antimicrobial peptides that differ in structure only by the orientation and spacial arrangement of the aromatic amino acids.

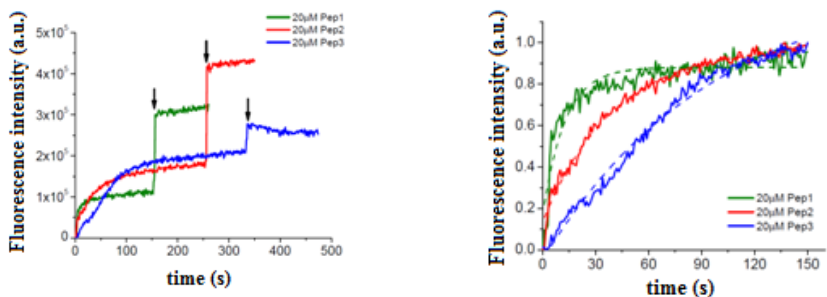


Fig.VIII.2.3.2 In left panel are shown typical traces of the fluorescence signal during experiments of calcein efflux from liposomes subjected to 20 μM of pep1 (green line), pep2 (red line) and pep3 (blue line). Solid vertical arrows indicate the maximum fluorescence value after addition of 25 μl of Triton X-100 (1%). In right panel are displayed normalized efflux functions caused by calcein release from liposomes exposed to identical aqueous concentrations of pep1 (green line), pep2 (red line) and pep3 (blue line) revealing the distinct kinetics of calcein efflux from liposomes interacting with peptides.

The kinetic of increase in fluorescence emission intensity of the released calcein upon mixing of pep1, pep2 and pep3 with vesicles, showed marked differences depending on the peptide used. While the model of peptide binding to liposomes can be elaborated within a simplified four-state model (e.g., peptide in solution, peptide bound to dye-filled liposomes, peptide in pore-forming configuration to liposomes, and peptide bound to empty liposomes) to provide values of the apparent rate constant of peptide binding (k_{app}), the fit of kinetic binding curves with a single exponential were used. The dashed lines are the fits of the experimental data to a simplified model $y(t) = y_0 + y_{\text{max}} e^{-k_{\text{app}} t}$, to provide apparent rate constant (k_{app}) of peptide binding. The values obtained demonstrated that pep1 ($k_{\text{app}} = 0.08 \text{ s}^{-1}$) was most effective in perturbing the liposomal membrane organization and releasing the entrapped calcein, as compared to pep2 ($k_{\text{app}} = 0.02 \text{ s}^{-1}$) and pep3 ($k_{\text{app}} = 0.01 \text{ s}^{-1}$), and this is in full agreement with electrophysiology experiments.

VIII.3. The study of peptides conformational changes in the presence of physiologically relevant metals

VIII.3.1. Langmuir mathematical model applied for determination of the dissociation constant between the peptide and copper ions

The Langmuir mathematical model. To further explore in a complementary fashion the effect of Cu^{2+} on the CAMA peptide conformation, with possible implications in explaining the data seen from single-molecule experiments, we recorded the intrinsic fluorescence spectra changes of the peptide given by its Trp 2, in the absence and presence of various amounts of Cu^{2+} . Steady-state fluorescence experiments revealed a sizeable blue shift of the fluorescence emission spectra of

Trp 2 residue from the primary structure of the CAMA peptide, corresponding to the change in wavelength of the maximum emission fluorescence signal of the peptide in the presence of variable amounts of Cu^{2+} , as compared to the Cu^{2+} - free spectrum. In accordance to the interpretation of similar data obtained with other peptides, this is a reasonable proof of a conformational change undergone by the CAMA peptide, which in the complexation with Cu^{2+} mostly at His 15 changes the microenvironment polarity around Trp 2, so that this amino acid becomes less exposed to the hydrophilic, water environment. To determine the expression that relates dissociation constant K_d , of the reversible interaction between Cu^{2+} and the CAMA peptide, we considered a simple bimolecular binding case between free peptides (P) and copper ions (Cu^{2+}), in which the two components bind reversibly to form a binary complex (P- Cu^{2+}). The dissociation constant K_d was extracted from the non-linear hyperbolic fit according to the equation:

$$\Delta\lambda = f\Delta\lambda_{\max} = \Delta\lambda_{\max} \frac{([P_0] + [Cu_0^{2+}] + K_d) - \sqrt{([P_0] + [Cu_0^{2+}] + K_d)^2 - 4[P_0][Cu_0^{2+}]}}{2[P_0]}$$

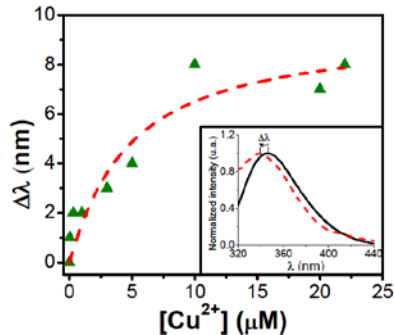


Fig.VIII.3.1.1 Bulk estimation of the affinity of Cu^{2+} towards the CAMA peptide measured at pH = 7. Upward triangles represent the blue shift of the fluorescence emission spectra of Trp 2 residue from the peptide ($\Delta\lambda$), corresponding to the change in wavelength of the maximum emission fluorescence signal of the peptide in the presence of various amounts of Cu^{2+} , as compared to the Cu^{2+} - free spectrum. The dashed line represent the non-linear hyperbolic fit ($R^2 = 0.88$), which provided an estimate of the dissociation constant of Cu^{2+} from the CAMA peptide ($K_d = 6.3 \mu\text{M}$). In the inset are displayed representative, normalized fluorescence emission spectra of the CAMA peptide [$1.5 \mu\text{M}$] in the absence of Cu^{2+} (continuous line) and in the presence of the maximum added Cu^{2+} ($[22 \mu\text{M}]$), dashed line), to evidence the blue shift of Trp 2 fluorescence emission spectra from the peptide.

VIII.3.2. The mathematical model developed for the study of association and dissociation reactions between the α - hemolysin pore and free- or Cu^{2+} -complexed CAMA peptide

In a first set of experiments, we probed the uni-molecular interaction between CAMA peptide added at micromolar concentration in the *trans* side of a membrane and a single *cis*-added α -HL protein.

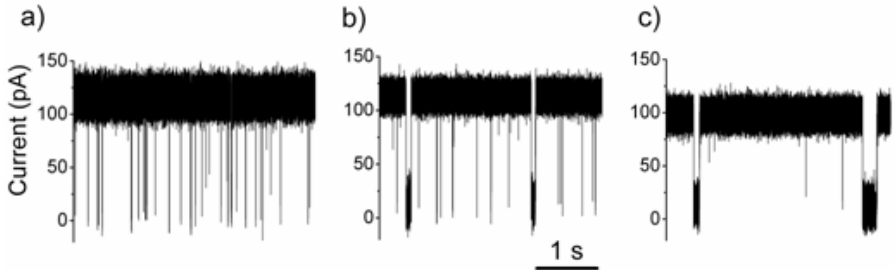


Fig. VIII.3.2.1 Typical electrophysiology recordings showing the effect of increasing copper ions concentration on the interaction of a single α -HL protein, with 30 μM CAMA peptide, in symmetrical 2M KCl solutions buffered at pH 7. In panels a, b and c are indicated selected traces showing the current fluctuations (downward spikes, from the initially fully open α -HL pore) recorded at +70 mV through a single α -HL pore mediated by its reversible interaction with a single peptide in the absence of Cu^{2+} (control, panel a), and in the presence of 10 μM (panel b), and respectively of 100 μM (panel c) *trans*-added Cu^{2+} .

In the absence of any interaction with the peptide, the α -HL protein pore is considered to be in the open state. The nanopore can undergo a change from open state to close state by interacting with the copper-free CAMA peptide (denoted by P) leading to the generation of a first type of blockage or with the copper-complexed CAMA peptide (denoted by P- Cu^{2+}) generating the second type of blockage.

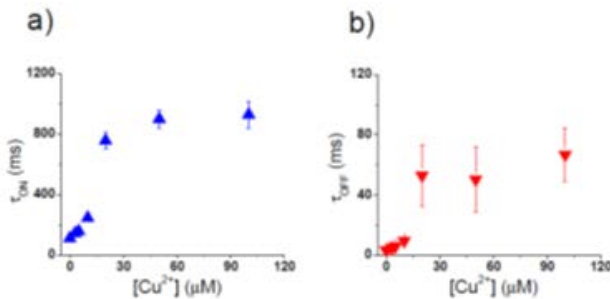


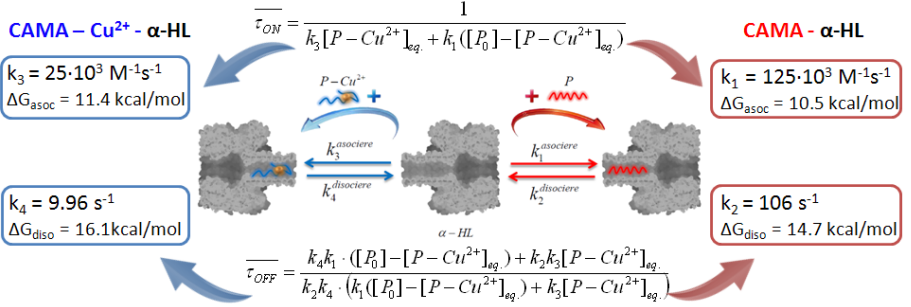
Fig. VIII.3.2.2 Quantitative analysis of the average time intervals which reflect the association (τ_{ON} ; panel a) and dissociation (τ_{OFF} ; panel b) of a single CAMA peptide in interaction with an α -HL protein at pH = 7, measured at various concentrations of Cu^{2+} (i.e., 0, 3, 5, 10, 20, 50 and 100 μM) added on the membrane *trans* side.

In a simplified way, the reactions that can take place at the single level in the protein nanopore, the mathematical reasoning based on the calculation of the probabilities of interaction between the peptide and the pore and the results of its application as well are represented in the figure below:

The dissociation constant between the CAMA peptide and the Cu^{2+} obtained from the spectroscopy fluorescence experiments:

$$K_d = 6.3 \mu\text{M}$$

$$[P - \text{Cu}^{2+}]_{\text{eq}} = \frac{([P_0] + [\text{Cu}_0^{2+}] + K_d) - \sqrt{([P_0] + [\text{Cu}_0^{2+}] + K_d)^2 - 4[P_0][\text{Cu}_0^{2+}]}}{2}$$



The analysis of the peptides volume inside the protein pore. The physical ground of this paradigm is very simple: the amplitude of the current blockages caused by a peptide (or protein) in interaction with a nanopore is directly proportional to the volume of peptide region which resides within the nanopore during the interaction, giving us the following relation:

$$\Delta I(t) = -\frac{\delta \cdot \sigma \cdot \Delta V \cdot w(t)}{l_{\text{por}}^2} \cdot \left[1 + \gamma \left(\frac{d_{\text{peptida}}}{d_{\text{por}}}, \frac{l_{\text{peptida}}}{l_{\text{por}}} \right) \right]$$

,where δ is a shape factor which equals 1 when the peptide inside the pore is viewed as a cylinder aligned parallel to the electric field lines, $v(t)$ (m^3) equals to the volume of

the peptide lodged within the pore, which may vary with time as the peptide moves across the pore, σ ($\Omega^{-1}\text{m}^{-1}$) is the conductivity of the electrolyte, ΔV is the potential difference imposed across the nanopore, and l_{pore} (m) equals the length of the nanopore, and the dimensionless correction factor, γ , which fine-tunes the formula above when the diameter of the peptide (d_{peptide}) equals the diameter of the pore (d_{pore}), or the length of the peptide (l_{peptide}) approaches the length of the pore (l_{pore}).

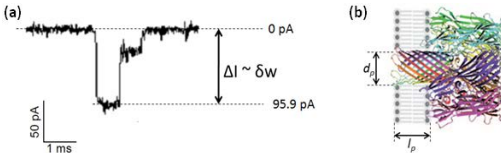


Fig. VIII.3.2.3 (a) Representation of the ionic current blockade (ΔI) generated by the transient passing of the CAMA peptide ($30 \mu\text{M}$) through the protein pore of α -HL. The amplitude of the blockade is directly proportional to the displaced volume of electrolyte solution (δw) inside the pore. (b) The assembled protein pore of α -HL into the lipid bilayer support.

In the absence of Cu^{2+} , by using estimates for the electrical conductivity of 2 M KCl ($\sigma = 169 \text{ mS cm}^{-1}$), the length of the α -HL pore region ($l_{\text{pore}} = 5.2 \text{ nm}$) and the average diameter of the α -HL β -barrel stem region ($d_{\text{pore}} = 1.5 \text{ nm}$), an average ion current blockage of $\Delta I = 95.9 \text{ pA}$ mediated by a peptide partially occluding the pore region of a protein clamped to a constant potential difference $\Delta V = 70 \text{ mV}$ corresponds to an excluded volume of electrolyte within the pore, by the lodged peptide, of $v \sim 3.3 \text{ nm}^3$. This indirectly approximates the value of the CAMA peptide volume, whose theoretically calculated value comes within a close range ($\sim 2.91 \text{ nm}^3$). Following a similar rationale, we estimated that in the presence of $100 \mu\text{M Cu}^{2+}$, the excluded volume of electrolyte within the nanopore by a temporarily residing peptide, seen experimentally as an average ion current blockage of $\Delta I = 79.4 \text{ pA}$ measured at the same potential difference equals $v(\text{CAMA}, 100 \mu\text{M Cu}^{2+}) \sim 2.74 \text{ nm}^3$. This difference in the amplitude of the ionic current blockade can be attributed to peptides conformational changes induced by the presence of copper ions, namely the coordination bond between the His15 amino acid from the peptides structure and the ion copper.

VIII.4. Human versus rat (1-16) fragments amyloid peptide in interaction with copper ions study

VIII.4.1. Single molecule study of the copper ion-induced conformational differences of human and rat amyloid peptides

When a peptide is added in the *trans* side of the lipid membrane in which a pore protein is inserted, and a potential is applied, it can be observed a series of blockades of the ionic current through the pore, due to the interactions occurring between the peptides and the lumen of the protein pore. The partial pore occlusion is due to the geometrical differences between the actual size of the peptide and the pore diameter, the passage of ions still being allowed but in a smaller amount generating ionic flux variation that can be registered and quantified.

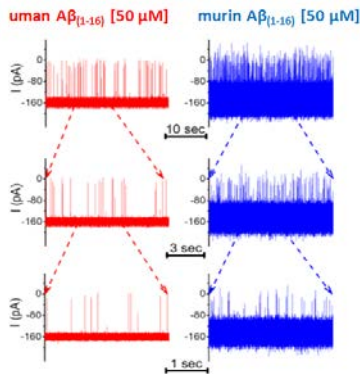


Fig.VIII.4.1.1 Representative ion current traces measured at $\Delta V = -100 \text{ mV}$ through a single α -HL protein, showing blockages induced by the human (left column) and rat (right column) $\text{A}\beta_{1-16}$ peptide added on the *trans* chamber at a concentration of $50 \mu\text{M}$. Due to the shorter blockage events induced by the rat $\text{A}\beta_{1-16}$ peptide, the cut-off frequency of the low-pass filter (f_c) was set at 20 kHz , as opposed to the case of the experiments involving the human $\text{A}\beta_{1-16}$ peptide where f_c was set at 10 kHz , and this is reflected by the increase in the noise of the traces showing the interaction between the rat $\text{A}\beta_{1-16}$ peptide and the protein pore.

The incremental increase of the added Cu^{2+} resulted in a decrease of number of events reflecting the peptide-induced blockages of the open pore current, and amplitude histogram analysis of the current fluctuations revealed that while in the absence of metal mostly one type of blockage event was seen (denoted by '#', Fig.VIII.4.1.2, panel e), supplementary peaks became visible (denoted by '&', Fig.VIII.4.1.2 panels g and h, and '\$', Fig.VIII.4.1.2 panels f and g) when the peptide was mixed in the trans chamber with various amounts of Cu^{2+} . The amplitude peak denoted by '*' reflects the average current through the un-blocked, peptide-free, α -HL pore. The extent of the current magnitude blockage induced by the peptide on the current flow through the protein (ΔI_{block}) is being quantified by the difference between the current measured in the absence of interaction (i.e., average values marked with '*') and the residual current through the protein hosting a single peptide (i.e., average values marked with '#') or '\$')

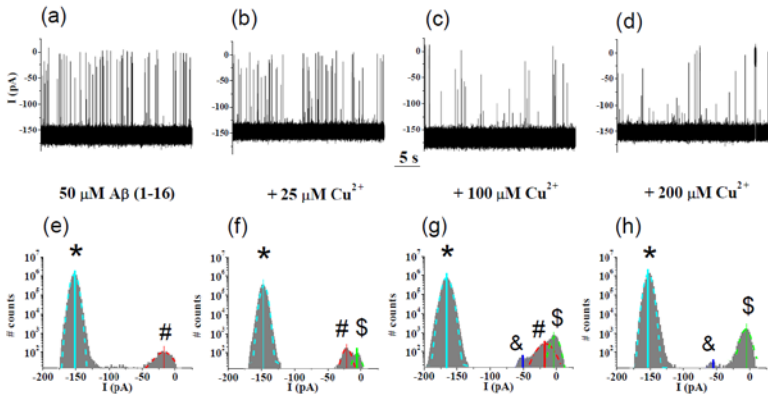


Fig.VIII.4.1.2 Typical single-channel current traces reflecting the uni-molecular interaction between the human $\text{A}\beta_{1-16}$ peptide with a α -HL pore, in the absence (panel a) and presence of *trans*-added Cu^{2+} at various concentrations (panels b, c and d), at an applied potential of -100 mV. Upward current spikes reflect the transient association of a single peptide with the protein pore, leading to a temporary occlusion of the ion permeating pathway through the pore, and therefore a reversible reduction in the magnitude of ion current flow. Data were recorded in the presence of 2 M KCl, 10 mM HEPES, pH=7.3, and the peptide concentration was 50 μM .

The quantitative analysis of the interactions kinetics of the the human amyloid peptides with the protein pore shows that the average time between two consecutive blocks (τ_{ON}) caused either by the free peptide or by the one complexed with copper ions (Fig.VIII.4.1.3, panel (e)), and also that the dwell time of the blockades (τ_{OFF}) (Fig.VIII.4.1.3, panel (f)) increases with the addition of copper ions concentration.

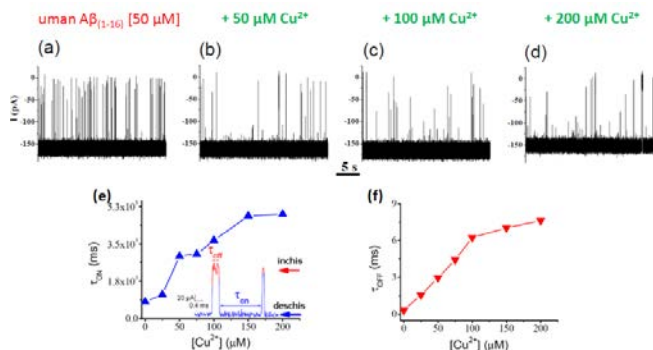


Fig.VIII.4.1.3 Analysis of the average dwell time intervals assigned the association (τ_{on} ; panel a) and dissociation (τ_{off} ; panel b) of a single human $A\beta_{1-16}$ peptide interacting reversibly with a α -HL pore, measured at various concentrations of the trans-added Cu^{2+} (i.e., 0, 25, 50, 75, 100, 150, and 200 μM).

Contrary to what was observed in the case of the human amyloid peptide (Fig.VIII.4.1.3), an increase in the concentration of copper ions leads to an increase in the events of pore blockage by the rat amyloid peptides (Fig.VIII.4.1.5).

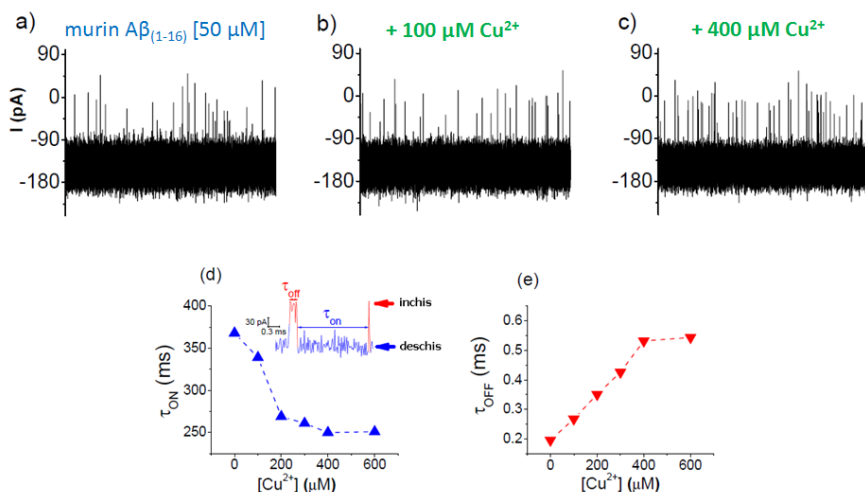


Fig.VIII.4.1.5 Representative single-channel current traces showing the uni-molecular interaction between the trans-added rat $A\beta_{1-16}$ peptide (50 μM) with a α -HL protein, in the absence of Cu^{2+} (panel a) and presence of *trans*-added Cu^{2+} (panel b; 100 μM , panel c; 400 μM), at an applied potential difference $\Delta V = -100$ mV. In panels below we show the outcome of the analysis on the average dwell time intervals assigned the association (τ_{on} ; panel d) and dissociation (τ_{off} ; panel e) of a single rat $A\beta_{1-16}$ peptide interacting reversibly with a α -HL pore, measured at various concentrations of the trans-added Cu^{2+} (i.e., 0, 100, 200, 300 and 400 μM).

Next, we have proposed a mathematical approach to estimate the numerical value of the dissociation constant (K_D), which describes the reversible reaction of amyloid peptide, of human origin or murin origin, and the copper ions.

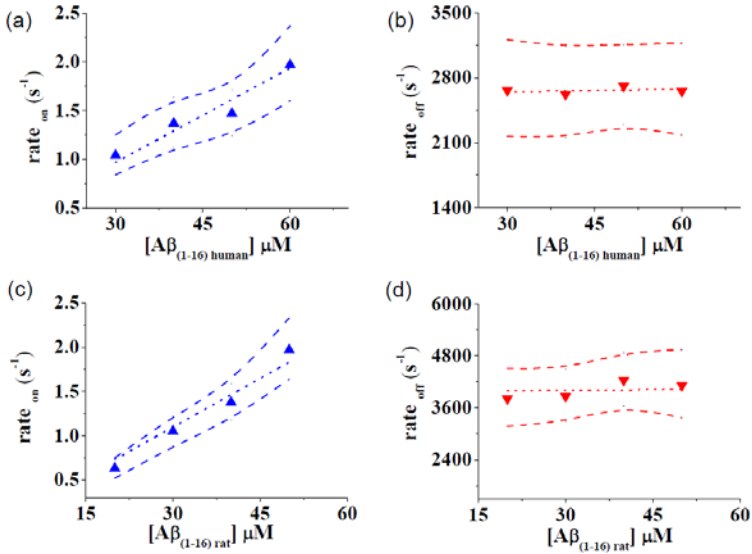
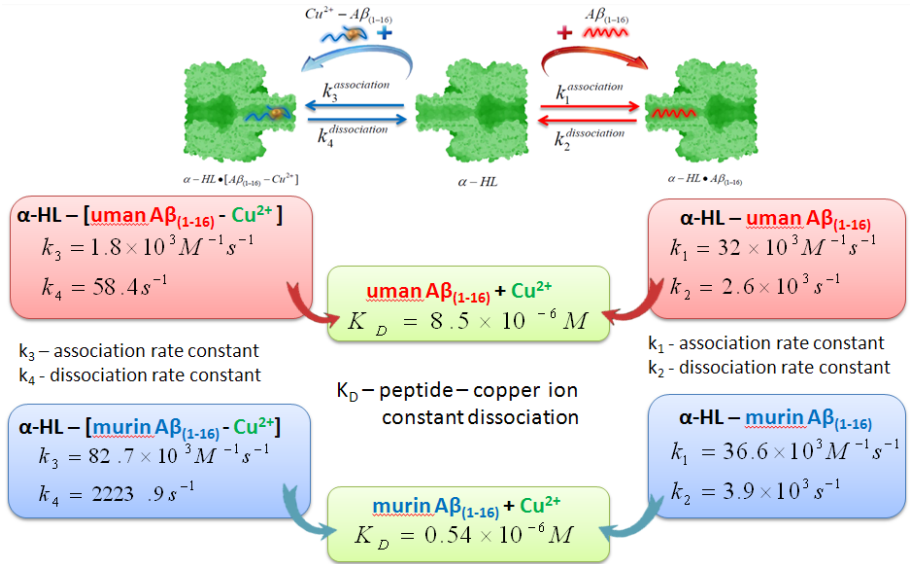


Fig.VIII.4.1.8 Quantitative kinetic description of the transient current blockages through the α -HL pore, induced by the interaction of the trans-added, human and rat $\text{A}\beta_{1-16}$ peptide, with the protein lumen. The frequency and duration of the human (panels a and b) and rat (panels c and d) $\text{A}\beta_{1-16}$ peptide-induced current blockades were analyzed within the statistics of exponentially distributed events. The inverse values of time constants corresponding to the in-between current blockage events as well as the average duration of blockage events provided quantitative estimations of the association (rate_{ON} , \blacktriangle) and dissociation (rate_{OFF} , \blacktriangledown) reaction rates that characterize the peptide – α -HL reversible interaction. The on rate constant was obtained from the slope of the linear fit of rate_{ON} vs peptide concentration (panel a, for the human $\text{A}\beta_{1-16}$ and panel c, for the rat $\text{A}\beta_{1-16}$). The off rate constant is independent of peptide concentration, and by virtue of the simple bimolecular model taken into account, it equals rate_{OFF} (panel b, for the human $\text{A}\beta_{1-16}$ and panel d, for the rat $\text{A}\beta_{1-16}$)

Based on the oversimplified formulations described above (subchapter VIII.3.2), the kinetic constants characterizing the reversible interactions between the human $\text{A}\beta_{1-16}$ peptides and the α -HL protein pore in the presence of added Cu^{2+} , were found: k_1 (human $\text{A}\beta_{1-16}$) = $26 \times 10^3 \pm 1.7 \times 10^3 \text{ s}^{-1}\text{M}^{-1}$, k_2 (human $\text{A}\beta_{1-16}$) = $3.1 \times 10^3 \pm 0.2 \times 10^3 \text{ s}^{-1}$, k_3 (human $\text{A}\beta_{1-16}$) = $4.1 \times 10^3 \pm 0.3 \times 10^3 \text{ s}^{-1}\text{M}^{-1}$, k_4 (human $\text{A}\beta_{1-16}$) = $131.6 \pm 9.5 \text{ s}^{-1}$. Following a similar line of reasoning, the kinetic constants describing the reversible interactions between the rat $\text{A}\beta_{1-16}$ peptide and the protein pore, in the presence of added Cu^{2+} , write: k_1 (rat $\text{A}\beta_{1-16}$) = $54.3 \times 10^3 \pm 4.3 \times 10^3 \text{ s}^{-1}\text{M}^{-1}$, k_2 (rat $\text{A}\beta_{1-16}$) = $4.4 \times 10^3 \pm 0.6 \times 10^3 \text{ s}^{-1}$, k_3 (rat $\text{A}\beta_{1-16}$) = $73 \times 10^3 \pm 5.6 \times 10^3 \text{ s}^{-1}\text{M}^{-1}$, k_4 (rat $\text{A}\beta_{1-16}$) = $2.04 \times 10^3 \pm 0.17 \times 10^3 \text{ s}^{-1}$.

In a simplified way, the reactions that can take place at the single level in the protein nanopore, the mathematical reasoning based on the calculation of the probabilities of interaction between the peptide and the pore and the results of its application as well are represented in the figure below:



VIII.5. Study of the physiologically relevant metals effect on the spatial conformation of human amyloid peptide 1-16 fragment

VIII.5.1. Single molecule study of human amyloid peptide 1-16 fragment in the presence of Cu^{2+} , Zn^{2+} , Fe^{3+} și Al^{3+} . Dissociation constant, K_D , between human amyloid peptide and metals ions determination

In this work, we employed electrical detection on a lipid membrane-immobilized $\alpha\text{-HL}$ protein nanopore, to quantify microscopic details underlying the interaction between Cu^{2+} , Zn^{2+} , Al^{3+} and Fe^{3+} and the human amyloid fragment $\text{A}\beta_{1-16}$. Our results support the proof-of-concept behind the possibility of using $\alpha\text{-HL}$ protein as a novel and potentially useful system to undertake a kinetic analysis of metals - amyloid- β ($\text{A}\beta$) peptide interactions, and estimate the equilibrium constants which characterize the reversible interactions between various metals and peptides. In a first set of experiments, we investigated at the uni-molecular level the interaction between the trans-added $\text{A}\beta_{1-16}$ peptides and a single cis-added $\alpha\text{-HL}$ protein, in the absence and presence of metals. When added on the trans side of a planar lipid membrane-containing an inserted $\alpha\text{-HL}$ protein, a negative potential in the trans side of the membrane facilitate the electrophoretic traffic of the human $\text{A}\beta_{1-16}$ peptides towards the $\alpha\text{-HL}$ protein, and the ensuing

peptide-protein interactions are seen as reversible blockages of the protein-mediated ionic current. The derivation of the kinetic constants which characterize the non-covalent $A\beta_{1-16} - \alpha$ -HL interactions are consistent with a simple bimolecular interaction between the peptide and the pore.

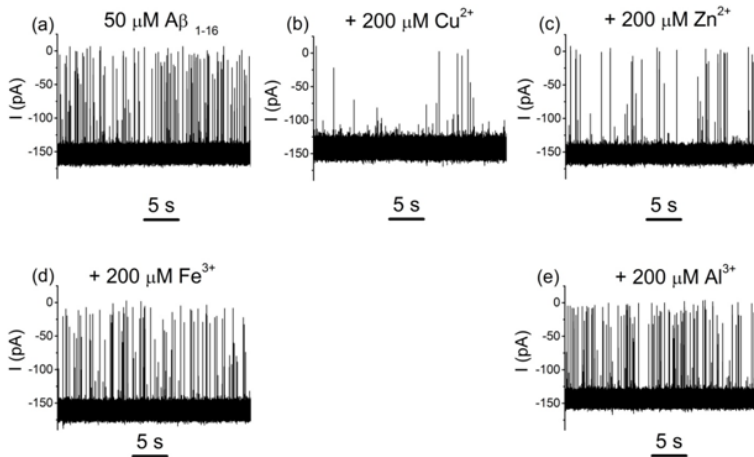


Fig.VIII.5.1.1 During the course of reversible interactions between the human $A\beta_{1-16}$ peptide and a single α -HL pore, the *trans*-chamber addition of Cu^{2+} , Zn^{2+} , Al^{3+} or Fe^{3+} led to distinct alterations in the kinetic fingerprint of blockade currents induced by the peptide from those in the absence of metals.

At the first glance, from such recordings it appears that unlike Cu^{2+} and Zn^{2+} , addition of Al^{3+} and Fe^{3+} entails a very slight change in the frequency of blockages caused by the $A\beta_{1-16}$ interaction with the α -HL pore. On the frame of a simple bimolecular interaction between the peptide and the pore, the inverse values of time constants corresponding to the free and occupied pore levels provided quantitative estimations of the association ($rate_{ON}$) and dissociation ($rate_{OFF}$) reaction rates that characterize the ‘metal - free’ $A\beta_{1-16} - \alpha$ -HL reversible interaction. Consequently, the on rate constant was obtained from the slope of the linear fit of $rate_{ON}$ vs. peptide concentration ($k_1=32 \times 10^3 \pm 1.1 \times 10^3 \text{ M}^{-1}\text{s}^{-1}$), while the off rate constants was independent of peptide concentration, and by virtue of the simple bimolecular model taken into account, equal $rate_{OFF}$ ($k_2=2.6 \times 10^3 \pm 17 \text{ s}^{-1}$). With these values estimations of dissociation constant values for Cu^{2+} and respectively Zn^{2+} binding to $A\beta_{1-16}$ were obtained ($K_d, Cu^{2+} = 4.5 \times 10^{-7} \text{ M}$, and $K_d, Zn^{2+} = 9.2 \times 10^{-5} \text{ M}$) which are qualitatively similar to values reported in the literature through other techniques.

Conclusions:

- The presence of phloretin quencher molecules cause an increase in the release percentage of calcein as a result of transmembrane pore formation by the melittin peptides.
- The probability of melittin peptide insertion and pore formation is favored at low ionic strength of the salt. This fact was observed both for the simple lipid systems and for the ones in which phloretin molecules were added.
- The pep1 peptides membranar activity is higher that in the case of the pep2 peptide, due to the higher energy cost required to insert into the hydrophobic core of the lipid membrane the peptide that contains two points of anchoring (pep2) compared to the peptide that has only one aromatic amino acid, meaning one point of anchoring to the membrane (pep1).
- The calculated difference in free energy of ~ 0.2 kcal/mol required to the peptides pore formation was attributed to cost of inserting into the hydrophobic core the aromatic amino acids W4 and F1 (pep2), positioned at the N-terminal, contrary to the one (W12) that is present in all the rest of the peptides, which is positioned at the C-terminal and remains anchored to the membrane.
- The lipid membrane affinity of the peptides with the most aromatic amino acids, distributed on both sides of the α -helix (pep2) is the highest. Also, W12 and W15 tryptophan amino acids of pep1 are oriented on the same side of the α -helix axis and have a higher affinity for the lipid membrane than pep3, which has the W12 and W13 tryptophan amino acids oriented on opposite sides of the α -helix.
- The histidine amino acid is the main binding site for the copper ions which has the highest affinity and also, its presence in the primary sequence of the CAMA peptide causes conformational changes due to the copper – histidine coordinative bonds that form.
- Due to the conformational changes undergo by the CAMA peptide after its interaction with the copper ions, the complex formed faces a higher energy barrier for associating with the protein pore, the free energy requirement being increased. Once the association is achieved, the interactions inside the pore are more energetically favorable, making the dissociation slower.

- In the presence of copper, both peptides show a high affinity for the α -hemolysin protein pore. The values obtained for the association and dissociation constants between the pore and the metal-complexed peptides, compared with those obtained for the interactions between the pore and the free-peptide can be attributed to a decrease in local hydrophobicity due to the conformational changes induced by the copper ions. However, given that the conformational changes induced by the copper ions on the human amyloid peptide produces a spatial rearrangement of the peptide so that the passage through the pore is more restricted, we may conclude that the increase in the local hydrophobicity is crucial for an increase in the affinity of the peptide for the pore. Also, although there are many factors which play a role in the development of Alzheimer's disease, this one may explain why the amyloid peptides found in mice do not aggregate in the presence of copper ions.
- The propensity of tested metals to interacting with the $A\beta_{1-16}$ peptide fragment inferred with the presented method was found obey the $Cu^{2+} > Zn^{2+} > Fe^{3+} > Al^{3+}$ series. The kinetic analysis of the frequency of blockage events entailed by $A\beta_{1-16}$ - α -HL interactions in the presence of metals with augmented affinity towards the peptide allowed us to quantify dissociation constants of Cu^{2+} and Zn^{2+} binding to the peptide.

The importance of determining the dissociation constant of amyloid peptide and physiologically relevant metal ions through the method developed in this thesis: Given that metal ions are known to play a critical role in β -amyloid neurotoxicity, investigations into the formation of metal- $A\beta$ complexes are of paramount interest, and easier to implement biophysical techniques like the one presented herein, may be productive in the study of biochemical aspects of metals binding to amyloid peptides. Our findings suggest that the presented technique should be able to complement analytical approaches aimed at unraveling the kinetics of various metals on β -amyloid interactions, and strengthen the feasible emergence of peptide-based metal sensors, through rational functionalizing of nanopores with peptide sequences suited for various metals recruitment and enhanced binding affinity.

Bibliography

- [1] J.I. Kourie et al., Properties of cytotoxic peptide-formed ion channels, 2000, *Am. J. Physiol. Cell Physiol.* 278, 1063-1087
- [2] M.S.P. Sansom et al., Ion channels formed by amphipathic helical peptides, 1991, *Eur. Biophys. J.* 20, 229-240
- [3] H.Sato et al., Peptide-membrane interactions and mechanisms of membrane destruction by amphipathic α -helical antimicrobial peptides, 2006, *BBA* 9, 1245-1256
- [4] D.W. Hoskin et al., Studies on anticancer activities of antimicrobial peptides, 2008, *BBA – Biomembranes* 1778, 357-375
- [5] Clarke, J., Wu, H., Jayasinghe, L., Patel, A., Reid, S. and Bayley, H. Continuous base identification for single-molecule nanopore DNA sequencing. *Nature Nanotechnology* 4, 265-270 (2009).
- [6] Garzon-Rodriguez, et al., Binding of Zn(II), Cu(II), and Fe(II) ions to Alzheimer's A beta peptide studied by fluorescence, *Bioorg Med Chem Lett.* 1999, 9(15), 2243-2248
- [7] Ha C, Ryu J, Park CB., Metal ions differentially influence the aggregation and deposition of Alzheimer's beta-amyloid on a solid template, *Biochemistry* 2007, 46(20), 6118-6125
- [8] Töugu V, et al, Binding of zinc(II) and copper(II) to the full-length Alzheimer's amyloid-beta peptide, *J Neurochem.* 2008, 104(5), 1249-12459
- [9] Atwood CS, et al., Dramatic aggregation of Alzheimer abeta by Cu(II) is induced by conditions representing physiological acidosis, *J Biol Chem.* 1998, 273(21), 12817-12826.
- [10] Vicente M. Aguilera et al., Lipid charge regulation of non-specific biological ion channels, *Phys. Chem. Chem. Phys.*, 2014,16, 3881-3893
- [11] H.Sato et al., Peptide-membrane interactions and mechanisms of membrane destruction by amphipathic α -helical antimicrobial peptides, 2006, *BBA* 9, 1245-1256
- [12] J. Antoinette Killian and Gunnar von Heijne, How proteins adapt to a membrane–water interface, *TIBS* 25 – SEPTEMBER 2000
- [13] D.A. Dougherty, Cation- π interactions in chemistry and biology: a new view of benzene, *peh, tyr and trp*, *Science, New Series* 1996, 271 (5246), 163-168
- [14] Stephen H White and William C Wimley, Peptides in lipid bilayers: structural and thermodynamic basis for partitioning and folding, *Current Opinion in structural biology* 1994 4:79-86
- [15] Gregg, E. C., Steidley, K. D., Kinetics of Cell Volume Changes of Murine Lymphoma Cells Subjected to Different Agents In Vitro, *Biophys. J.* 1965, 5, 393–405.
- [16] DeBlois, R. W.; Bean, Counting and sizing of submicron particles by resistive pulse technique, *C. P. ReV. Sci. Instrum.* 1970, 41, 909–916.
- [17] Bezrukov, S. M. J., Ion channels as molecular coulter counters to probe metabolite transport, *Membr. Biol.* 2000, 174, 1–13.
- [18] Deamer, D.; Branton, D., Characterization of nucleic acids by nanopore analysis , *Acc. Chem. Res.* 2002, 35, 817–825.

- [19] J. Clarke et al., Continuous base identification for single-molecule nanopore DNA sequencing, *Nat. Nanotechnol.* 2009, 4, 265–270.
- [20] Q. Zhao et al., Real-time monitoring of peptide cleavage using a nanopore probe, *J. Am. Chem. Soc.* 2009, 131, 6324–6325.
- [21] H. Wang et al., Peering into Biological Nanopore: A Practical Technology to Single-Molecule Analysis, *Chem. Asian J.* 2010, 5, 1952–1961.
- [22] David S. Talaga and Jiali Li, Single-Molecule Protein Unfolding in Nanopores, *J. Am. Chem. Soc.* 2009, 131, 9287–9297
- [23] L.Z. Song et al., Structure of staphylococcal alpha-hemolysin, a heptameric transmembrane pore., 1996, *Science* 274, 1859–1866
- [24] S.-H. Shin et al, Kinetics of a reversible covalent-bond forming reaction observed at the single molecule level., 2002, *Angew. Chem. Int. Edit.* 41, 3707-3709
- [25] O. Braha et al., H. Simultaneous stochastic sensing of divalent metal ions, 2000, *Nature Biotechnology* 18, 1005-1007
- [26] X. Guan et al., Stochastic sensing of TNT with a genetically engineered pore, 2005, *ChemBioChem* 6, 1875-1881
- [27] J.J. Kasianowicz et al., Characterization of individual polynucleotide molecules using a membrane channel., 1996, *Proc. Natl. Acad. Sci. USA* 93, 13770–13773
- [28] A. Meller et al., Rapid nanopore discrimination between single polynucleotide molecules., 2000, *Proc. Natl. Acad. Sci. USA* 97, 1079-1084
- [29] C. James et al., Continuous base identification for single-molecule nanopore DNA sequencing., 2009, *Nature Nanotechnology* 4, 265-270
- [30] A.J. Wolfe et al., Catalyzing the translocation of polypeptides through attractive interactions., 2007, *J. Am. Chem. Soc.* 129, 14034-14041
- [31] L. Movileanu et al., Interaction of peptides with a protein pore, *Biophys. J.* 2005, 89, 1030–1045
- [32] Q. Zhao et al., Study of Peptide Transport through Engineered Protein Channels, 2009, *J. Phys. Chem. B* 113, 3572–3578
- [33] Ayumi Hirano-Iwata et al., The design of molecular sensing interfaces with lipid bilayer assemblies, 2008, *Trends in analytical chemistry* 27(6), 512-520
- [34] Danielsson, J., Pierattelli, R., Banci, L. & Graslund, A. (2007). High-resolution NMR studies of the zinc-binding site of the Alzheimer's amyloid β -peptide, *FEBS Journal*, 274, pp. 46-59.
- [35] Gaggelli, E., Janicka-Klos, A., Jankowska, E., Kozlowski, H., Migliorini, C., Molteni, E., Valensin, D., Valensin, G., & Wieczorzak, E. (2008). NMR Studies of the Zn^{2+} Interactions with Rat and Human β -Amyloid (1-28) Peptides in Water-Micelle Environment, *Journal of Physical Chemistry B*, 112, 100-109.
- [36] M.A. Lovell, et al., Copper, iron and zinc in Alzheimer's disease senile plaques, *J Neurol Sci.* 1998, 158, 47–52
- [37] E. Burstein et al., Decomposition of protein tryptophan fluorescence spectra into log-normal components. I. Decomposition algorithms, 2001, *Biophys. J.* 81, 1699 - 1709
- [38] J.R. Lakowicz, *Principle of fluorescence spectroscopy*, 2006 3rd edition, Springer Science + Business Media, LLC, New York
- [39] T. Ruysschaert et al., Liposome retention in size exclusion chromatography, 2005, *BMC Biotechnology* 1186/1472
- [40] L. Silvestro et al., The Concentration-Dependent Membrane Activity of Cecropin A, 1997, *Biochemistry* 36, 11452-11460

- [41] Eftink MR, Ghiron C. 1981. Fluorescence quenching studies with proteins. *Anal Biochem* 114:199–227.
- [42] Eftink MR. 1991. Fluorescence quenching reactions: probing biological macromolecular structures. In *Biophysical and biochemical aspects of fluorescence spectroscopy*, pp. 1–41. Ed TG Dewey. Plenum Press, New York.
- [43] Eftink MR. 1991. Fluorescence quenching: theory and applications. In *Topics in fluorescence spectroscopy, Vol. 2: Principles*, pp. 53–126. Ed JR Lakowicz. Plenum Press, New York.
- [44] M.V. Frassa et al., A. Structure and stability of the neurotoxin PV2 from the eggs of the apple snail *Pomacea canaliculata*, *Biochim. Biophys. Acta* 2010, 1804 (7), 1492–1499

SCIENTIFIC ACTIVITY:

1. Articles published in scientific journals with an impact factor (ISI):

1. Alina Asandei, Sorana Iftemi, Loredana Mereuta, **Irina Schiopu** and Tudor Luchian, *Probing of Various Physiologically Relevant Metals–Amyloid- β Peptide Interactions with a Lipid Membrane-Immobilized Protein Nanopore*, 2014, The journal of membrane biology, 247 (6), pp. 523 - 530
IF: 2.478
First autor: no, coautor
2. Alina Asandei*, **Irina Schiopu***, Sorana Iftemi, Loredana Mereuta and Tudor Luchian, *Investigation of Cu²⁺ Binding to Human and Rat Amyloid Fragments A β (1–16) with a Protein Nanopore*, 2013, Langmuir, 29 (50), pp. 15634 – 15642
IF: 4.186
First autor: yes, equal contributions with CS III Dr. Alina Asandei
3. Loredana Mereuta*, **Irina Schiopu***, Alina Asandei, Yoonkyung Park, Kyung-Soo Hahm, Tudor Luchian, *Protein nanopore-based, single-molecule exploration of copper binding to an antimicrobial-derived, histidine-containing chimera peptide*, 2012, Langmuir, 28 (49), pp. 17079 – 17091
IF: 4.186
First autor: yes, equal contributions with Lect. Univ. Dr. Loredana Mereuta
4. **Irina Schiopu***, Loredana Mereuță*, Aurelia Apetrei, Yoonkyung Park, Kyung-Soo Hahm, Tudor Luchian, *The role of tryptophan spatial arrangement for antimicrobial-derived, membrane-active peptides adsorption and activity*, 2012, Molecular BioSystems, 8 (11), pp. 2860 - 2863
IF: 3.534
First autor: yes, equal contributions with Lect. Univ. Dr. Loredana Mereuta

2. Papers presented at international conferences

1. **Irina Schiopu**, Alina Asandei, Sorana Iftemi, Loredana Mereuta, Liliana Chiribasa, Tudor Luchian, *Single – molecule probing of Cu²⁺ induced folding on human versus rat amyloid A β (1-16) fragments*, IC-ANMBES 2014, Brasov, Romania, 13 – 15 June 2014 (**poster presentation**)

2. **Irina Șchiopu**, Loredana Mereuță, Alina Asandei, Tudor Luchian, *Copper(II) binding to a histidine - containing chimera peptide: a single protein nanopore study*, FEBS Workshop: Biological surfaces and interfaces, Sant Feliu de Guixols, Catalonia, Spain, 30 June – 5 July 2013 (**poster presentation**).
3. **Irina Șchiopu**, Loredana Mereuță, Aurelia Apetrei, Tudor Luchian, *Electrophysiology and fluorescence studies of the key role played by the position of aromatic amino acids in antimicrobial peptide activity and translocation*, 9th ISCBPU, International Student Conference of Balkan Physical Union, Constanța, România, 5-7 July 2012 (**oral communication**).
4. Aurelia Apetrei, **Irina Șchiopu**, Loredana Mereuță, Tudor Luchian, *Electrophysiology study of amyloid beta channel formation and activity in reconstructed planar lipid membranes*, 8th BPU, The 8th General Conference of Balkan Physical Union, Constanța, România, 5-7 July 2012 (**poster presentation**).
5. **Irina Șchiopu**, Loredana Mereuță, Aurelia Apetrei, Tudor Luchian, *Tryptophan anchor position determines antimicrobial peptide activity and translocation*, Third International Symposium on Antimicrobial Peptides – “Today knowledge and future applications”, Lille, Franța, 13-15 June 2012 (**poster presentation**).

3. Papers presented at national conferences

1. Liliana Chiribasa, **Irina Șchiopu**, Tudor Luchian, *The modulatory effects exerted by electrical properties of lipid membranes and ionic strength upon peptides - biomimetic systems interactions*, FTEM National Conference, Iași, 26 October 2013 (**oral communication**).
2. **Irina Șchiopu**, Loredana Mereuță, Alina Asandei, Tudor Luchian, *Analysis of copper ion induced peptide folding through a nanopore sensing technique*, 12th National Conference on Biophysics „CNB 2013” – Biophysics of Health, with *international participation*, Iași, 13-16 June 2013 (**oral communication**).
3. Liliana Chiribașa, **Irina Șchiopu**, Tudor Luchian, *Mellitin affinity enhancement through a dipole potential modifying agent*, 12th National Conference on Biophysics „CNB 2013” – Biophysics of Health, with *international participation*, Iași, 13-16 June 2013 ((**poster presentation – Best Poster Prize**)).
4. Liliana Chiribașa, **Irina Șchiopu**, Tudor Luchian, *Importanța aminoacidului Triptofan în studiul adsorbției peptidei antimicrobiene melitină*, National Conference on Fundamental and Applied Research in Physics, Iași, 26 October 2012 (**poster presentation**).

5. Liliana Chiribaşa, **Irina Şchiopu**, Tudor Luchian, *Tryptophan fluorescence study of the adsorption of antimicrobial peptide Melitin*, FTEM National Conference, Iaşi, 12 – 14 May 2012 (**oral communication – 1st Prize**)
6. **Irina Schiopu**, Aurelia Apetrei, Tudor Luchian, *The modulatory role of cholesterol on the activity of the antimicrobial peptide Cecropin B: a fluorescence approach*, National Conference of Biophysics, Sibiu, 10-12 November 2011 (**poster presentation – Best Poster Prize**)

4. Research grants

1. **PN-II-ID-PCCE-2011-2-0027/01.06.2012** - BIOSENS: „ *Ion sensing and separation through modified cyclic peptides, cyclodextrines and protein pores* ”
2. **PN-II-PT-PCCA-2011-3.1-0595** - BIOPEP: „ *Rational design and generation of synthetic, short antimicrobial peptides. Linking structure to function*”